Catalysis Science & Technology

Accepted Manuscript

ROYAL SOCIETY OF CHEMISTRY

www.rsc.org/catalysis

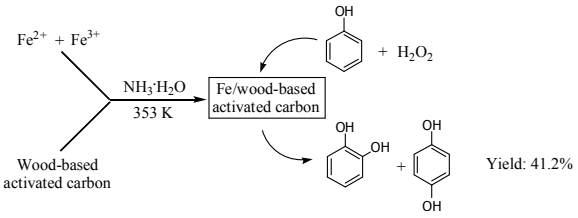

The loading of Fe^{3+} and Fe^{2+} on wood-based activated carbon obtained Fe-based catalyst with good catalytic performance for phenol hydroxylation.

Catalysis Science & Technology RSCPublishing

ARTICLE

The preparation of Fe/wood-based activated carbon catalyst for phenol hydroxylation from Fe^{2+} and Fe^{3+} precursors†

Ruiguang Yang, Guiying Li*, and Changwei Hu*

Cite this: DOI: 10.1039/xoxxoooooox

Received ooth January 2012,
Accepted ooth January 2012

DOI: 10.1039/xoxxoooooox

www.rsc.org/

A series of Fe/wood-based activated carbon catalysts with 0.89-6.94 wt% Fe loading were prepared using impregnation-co-precipitation method, and the catalysts were characterized by inductively coupled plasma, N_2 adsorption-desorption, X-ray diffraction, X-ray photoelectron spectroscopy, magnetic measurements, ultraviolet-visible diffuse reflectance spectroscopy, fourier transform infrared spectroscopy and high resolution transmission electron microscopy. The results indicated that iron oxide species including Fe^{2+} and Fe^{3+} forming the active sites were successfully loaded on wood-based activated carbon. With increasing concentration of iron ions in the preparation process, iron oxide species were saturated gradually on the support. These catalysts have been assessed for the hydroxylation of phenol to dihydroxybenzenes using H_2O_2 as oxidant. The results showed that the catalytic activity was improved with the increase of Fe content. The active phase for phenol hydroxylation could be the cooperation of the two iron oxide species. Under the optimized conditions, the catalyst with an Fe content of 6.55 wt% gave a phenol conversion of 51.1% with 80.6% of selectivity to dihydroxybenzenes. Finally, the results of catalyst recycling illustrated that the catalyst could be reused with slight Fe leaching and slight loss of activity.

1 Introduction

Hydroquinone (HQ) and catechol (CAT), as important chemical materials and intermediates, have been widely used in photographic developer, pharmaceutics, polymerization inhibitor, antioxidant, and so on.[1-4] The heterogeneous catalytic hydroxylation of phenol to produce dihydroxybenzenes (DHB, that is, HQ and CAT) with H_2O_2 as oxidant, has attracted much attention due to the favorable properties of solid catalysts. In recent years, there has been growing research interest in finding suitable solid catalysts, especially those containing transition metal ions, for the hydroxylation of phenol to DHB under mild reaction conditions, with clean oxidants like O_2 and H_2O_2. Efforts are made to use various materials, such as zeolites[5-7], mesoporous materials[8-11], hydrotalicite-like compounds[12-14], nanoparticles[15-17], and so on. Li et al. have prepared microporous carbon molecular sieve for the titled reaction and obtained a phenol conversion of 29.6% with selectivity of 85.1% to DHB.[18] Among the transitional metals studied, Fe showed the best activity. Therefore, much attention has been paid to the development of Fe-containing catalysts. Adam et al. have hydrothermally synthesized Fe modified zeolite L nanocrystals, which gave a phenol conversion of 93.40% in the presence of acetic acid in 30 min.[19] Liang et al. have prepared mesoporous Fe-incorporated materials, which gave a phenol conversion of 47.3%.[20]

Activated carbon (AC) is a general adsorbent of organic compounds from aqueous solutions with huge surface area and abundant porosity.[21] Apart from adsorbent, AC can also act as a heterogeneous catalyst or catalytic support. Because of the presence of surface oxygen functional groups, AC has been found useful in catalysis.[22] It is well-known that large surface area and high porosity are helpful for the dispersion of active phases, which results in the increase of catalytic activity. It means that AC may be an excellent catalyst support. Jin et al. have applied Fe/AC as a catalyst to directly convert phenol to DHB, and a phenol conversion of 41.3% with DHB yield of 36.0% was obtained.[2] It was proposed that high catalytic activity was mainly attributed to the efficient catalytic component, Fe_3O_4, which formed by ferric species partly reduced to ferrous species over AC at 673 K in air.

Taking these factors into consideration, we loaded Fe on the wood-based activated carbon (WAC) by the use of both Fe^{2+} and Fe^{3+} in the preparation process in an attempt to obtain high activity catalyst for the hydroxylation of phenol.

2 Experimental

2.1 Materials used

Commercially available WAC (40-60 mesh) was provided by Jiangsu Nantong Activated Carbon Cooperation (China). Prior to use, WAC was washed three times by deionized water and dried at 383 K for 24 h. Ferric nitrate ($Fe(NO_3)_3 \cdot 9H_2O$) and ferrous sulfate ($FeSO_4 \cdot 7H_2O$) were used as the precursors of Fe. $NH_3 \cdot H_2O$ (1 mol/L) and glacial acetic acid were used to adjust the pH value. Phenol and 30 wt% H_2O_2 (Kelong, Chengdu, China) were used as the materials for catalytic

activity test.

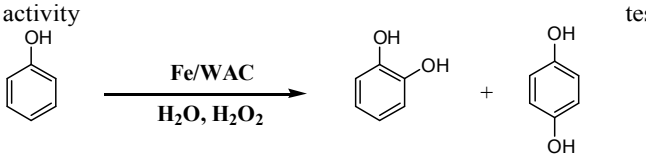

Phenol **Catechol** **Hydroquinone**

Scheme 1 Catalytic phenol hydroxylation by H_2O_2

Table 1 The content of Fe in catalysts

Concentration of iron ions [a] (mol/L)	Fe content of catalysts (wt%)
0.018	0.89
0.054	2.76
0.108	4.82
0.162	6.55
0.198	6.94

[a] Iron ions included Fe^{2+} and Fe^{3+}, and the molar ratio of Fe^{3+} to Fe^{2+} was 2:1.

All the solvents and reagents were commercially available with analytical purity (purity > 99%).

2.2 Preparation of catalysts

The impregnation-co-precipitation method used for the preparation of Fe/wood-based activated carbons (Fe/WACs) was similar to that reported in literatures[23-24]. 5 g of WAC was impregnated with 50 ml of aqueous solution of $Fe(NO_3)_3 \cdot 9H_2O$ and $FeSO_4 \cdot 7H_2O$ with desired concentrations (the molar ratio of Fe^{3+} to Fe^{2+} being controlled to be 2:1) for 30 min under N_2 atmosphere. The mixture was heated to 353 K and 1 mol/L $NH_3 \cdot H_2O$ was added continuously to adjust the pH to 9 under vigorous stirring. Then the sample was stirred and kept at 353 K for 1 h. The product was washed by deionized water (until the pH being 7), and dried at 353 K in a vacuum oven for 24 h. The obtained samples were sieved to obtain the 40-60 mesh catalysts and referred to Fe/WAC/*x* (*x* was the actual Fe content of the catalysts from the ICP-AES results).

2.3 Characterization of the catalysts

The actual Fe content loaded on the catalysts in the catalytic hydroxylation process was determined by inductively coupled plasma-atomic emission spectrometer (ICP-AES).

The textural characterization of the catalyst was performed by N_2 physisorption at liquid nitrogen temperature (77 K) using a Micromeretics Tristar 3020 automatic analyzer. Prior to the measurements, samples were degassed at 573 K for 4 h under vacuum. The surface area (S_{BET}) was determined by BET method, and the specific surface area of the micropores (S_{mic}) and micropore volume (V_{mic}) were calculated by the t-plot method. The pore size distributions were calculated by DFT method.

X-ray diffraction (XRD) patterns were obtained on a diffractometer (LTD DX-1000 CSC) using Cu K_α (λ = 1.54056 Å) radiation. The apparatus was operated at 25 mA and 40 kV. The data were collected with a step of 0.0544°, using continuous scanning mode in the range of $10 \le 2\theta \le 80^o$.

X-ray photoelectron spectroscopy (XPS) was taken with an AXIS Ultra DLD (KRATOS) spectrometer with Al K_α radiation (1486.6 eV). The binding energy scale was calibrated with respect to the adventitious carbon (C 1s) at 284.6 eV. The data were analyzed with the use of standard software. A Shirley background was subtracted from all spectra.

The magnetic property was studied by a vibrating sample magnetometer (Lake Shore 7410) at room temperature.

Ultraviolet-visible diffuse reflectance (DR UV-vis) spectra were obtained in the range from 200 to 800 nm using a UV-3600 spectrometer equipped with a reflectance attachment. $BaSO_4$ was used as the reference material.

Fourier transform infrared (FTIR) spectra were collected at 2 cm^{-1} resolution using a Nicolet Nexus 670 FTIR spectrometer equipped with a mercury cadmium telluride detector.

High resolution transmission electron microscopy (HRTEM) images were obtained with an FEI Company Tecnai G2[20] Stwin instrument operated at 200 kV. The samples were ultrasonically dispersed in ethanol at room temperature for 30 min. The as-obtained solutions were dropped onto copper grids for TEM.

2.4 Phenol hydroxylation reaction

Phenol hydroxylation was catalyzed by Fe/WACs in water. The analysis of the reaction mixture demonstrated that the main products were CAT and HQ (Scheme 1). The main by-products were p-benzoquinone (BQ) and polymeric tars. In most cases, tars were not directly detectable, and the presence of tars in the reaction mixture was identified by mass balance.[17]

The investigation of the catalytic activity was carried out by the following procedure: the reaction was performed in a 50 ml two-necked round-bottom flask, equipped with a magnetic stirrer, a reflux condenser and a temperature controllable water-bath. In a typical run, 0.48 g of phenol (5 mmol), 10.00 g of water, 0.26 g of acetic acid, and 0.05 g of catalyst were added to the reactor and the system was stirred at 313 K. To start the reaction, 0.50 g of 30 wt% H_2O_2 solution (5 mmol) was added at once. The reaction products were collected, identified, and quantified by high performance liquid chromatography (HPLC, Comatex C18 column, 4.6 mm i.d. × 250 mm), using UV detector at 277 and 254 nm. The conversion of phenol (X_{Ph}), the selectivity to DHB (S_{DHB}), the yield of products or by-products (Y_{DHB}, Y_{CAT}, Y_{HQ}, Y_{BQ} and Y_{Others}), and the effective utilization of H_2O_2 ($U_{H_2O_2}$) were defined as follows:

$$X_{Ph} = (n^0_{Ph} - n_{Ph})/n^0_{Ph} \times 100\%$$

$$S_{DHB} = (n_{CAT} + n_{HQ})/(n^0_{Ph} - n_{Ph}) \times 100\%$$

$$Y_{DHB} = (n_{CAT} + n_{HQ})/n^0_{Ph} \times 100\%$$

$$Y_{CAT} = n_{CAT}/n^0_{ph} \times 100\%$$

$$Y_{HQ} = n_{HQ}/n^0_{Ph} \times 100\%$$

$$Y_{BQ} = n_{BQ}/n^0_{Ph} \times 100\%$$

$$Y_{Others} = (n^0_{Ph} - n_{Ph} - n_{CAT} - n_{HQ} - n_{BQ})/n^0_{Ph} \times 100\%$$

$$U_{H_2O_2} = (n_{CAT} + n_{HQ} + 2n_{BQ})/n^0_{H_2O_2} \times 100\%$$

Where n^0_{Ph} and n_{Ph} denoted the initial and final amounts (moles) of phenol, respectively, and $n^0_{H_2O_2}$ denoted the initial amount (moles) of hydrogen peroxide, while n_{CAT}, n_{HQ} and n_{BQ} denoted the produced amounts (moles) of CAT, HQ and BQ,

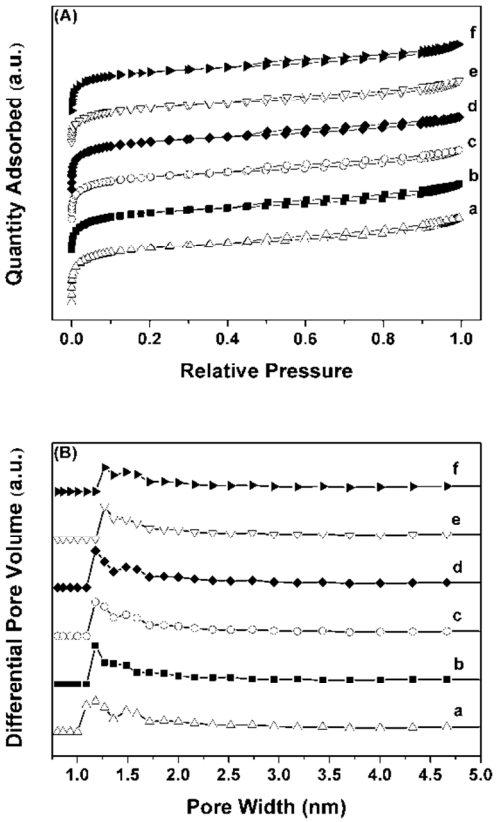

Fig. 1 N_2 adsorption-desorption isotherms (A) and pore size distributions (B) of catalysts: (a) WAC, (b) Fe/WAC/0.89, (c) Fe/WAC/2.76, (d) Fe/WAC/4.82, (e) Fe/WAC/6.55, (f) Fe/WAC/6.94.

Table 2 The structural properties of Fe/WAC samples

Catalyst	S_{BET} (m^2/g)	S_{mic} (m^2/g)	V_t (cm^3/g)	V_{mic} (cm^3/g)	V_{mic}/V_t (%)
WAC	922	769	0.51	0.30	58.8
Fe/WAC/0.89	912	759	0.49	0.30	61.2
Fe/WAC/2.76	896	745	0.48	0.29	60.4
Fe/WAC/4.82	873	721	0.46	0.28	60.9
Fe/WAC/6.55	844	690	0.46	0.27	58.7
Fe/WAC/6.94	838	683	0.45	0.27	60.0

respectively. The subscript "Others" denoted the sum of tars formed.

3 Results and discussion

3.1 Characterizations of the catalysts

3.1.1 The ICP-AES analysis

The Fe content of the catalysts before reaction was shown in Table 1. When the concentration of iron ions (total concentrations of Fe^{3+} and Fe^{2+}) increased from 0.018 to 0.162 mol/L, the Fe content of the catalysts monotonically increased from 0.89 to 6.55 wt% accordingly.

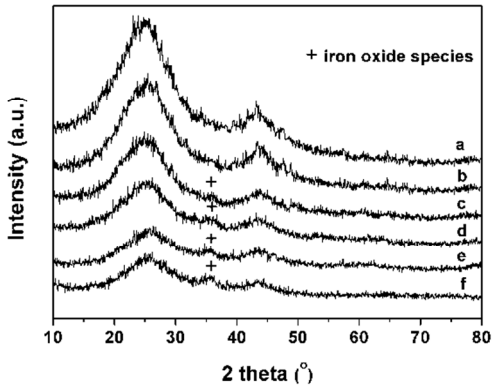

Fig. 2 The X-ray diffraction patterns of samples: (a) WAC, (b) Fe/WAC/0.89, (c) Fe/WAC/2.76, (d) Fe/WAC/4.82, (e) Fe/WAC/6.55, (f) Fe/WAC/6.94.

However, when the concentration of iron ions exceeded 0.162 mol/L, the Fe content of the catalyst changed slightly. Visually, there were a lot of black isolated granules belonged to iron oxides apart from the WAC after the co-precipitation process. The results illustrated that with high concentration of iron ions, a lot of isolated iron oxides were not loaded on WAC after the saturated adsorption of Fe^{2+} and Fe^{3+} on WAC. It implied that the Fe loading depended on the nature of WAC under the present preparation conditions.

3.1.2 The N_2 adsorption-desorption isotherms

Fig. 1 showed the N_2 adsorption-desorption isotherms and pore size distributions of WAC and Fe/WACs. WAC exhibited type I eminent characteristic of the microporous material. It was clear that Fe/WACs had similar N_2 adsorption-desorption isotherms to that of WAC. Obviously, Fig. 1 (B) showed that all samples possessed heterogeneous micropores, and some small micropores disappeared with increasing Fe content. The structural properties of Fe/WAC samples were listed in Table 2. The S_{BET}, S_{mic}, V_t, and V_{mic} slightly decreased with increasing Fe content, but the V_{mic}/V_t nearly kept unchanged. Thus, the textural parameters of the Fe/WACs were not significantly different from WAC. Because of the low Fe content, it was assumed that Fe loading did not influence significantly the textural parameters of the support in the preparation process of catalyst.

3.1.3 The XRD patterns

The XRD patterns of all the samples were presented in Fig. 2. Interestingly, as Fe loading increased from 2.76 to 6.94 wt%, only a broad peak appeared with increased intensity at 35.6°. Although Fe_3O_4 was designed to form on WAC in the preparation process of the catalyst, it was difficult to assert the formation of Fe_3O_4 (18.3°, 30.1°, 35.5°, 43.1°, 62.6°) or Fe_2O_3 (23.2°, 32.9°, 35.7°, 49.4°, 53.3°)[24]. Anyway, the peak should be attributed to the existence of iron oxide species. The XRD pattern of low Fe loading sample (Fe/WAC/0.89) was similar to that of WAC. The diffused character of low-intensity diffraction peak was indicative of the high dispersion of iron oxide species, which might be caused by the interaction of the surface groups of WAC with iron ions. The huge

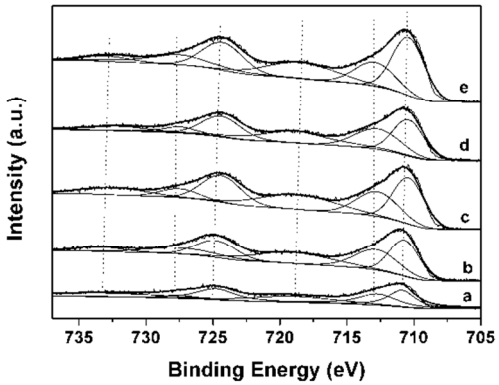

Fig. 3 Fe2p spectra of catalysts: (a) Fe/WAC/0.89, (b) Fe/WAC/2.76, (c) Fe/WAC/4.82, (d) Fe/WAC/6.55, (e) Fe/WAC/6.94.

Table 3 Surface compositions of samples determined by XPS

Catalyst	Fe^{3+}/Fe^{2+} (molar ratio)	Fe [a] (atom.%)	O [b] (atom.%)	Fe/O (%)
Fe/WAC/0.89	0.63	4.71	16.85	0.28
Fe/WAC/2.76	0.61	7.88	26.14	0.30
Fe/WAC/4.82	0.52	11.80	38.47	0.31
Fe/WAC/6.55	0.52	12.86	41.05	0.31
Fe/WAC/6.94	0.50	13.79	43.30	0.32

[a] Fe meant the whole iron present on the surface.
[b] O meant the whole oxygen present on the surface.

surface of WAC and the interaction between iron ions and surface groups of WAC might prevent the formation of crystal iron oxides. This might be the reason for the saturation of Fe loading.

3.1.4 The XPS analysis

Fig. 3 showed the Fe 2p spectra of the Fe/WACs samples. Surface analysis by XPS confirmed the presence of Fe^{3+} and Fe^{2+} on Fe/WACs, on the basis of the Fe 2p peak position and the energy difference between the Fe $2p_{1/2}$ excited state and the Fe $2p_{3/2}$ ground state.[25] After deconvolution, the peaks at 710.7 and 712.7 eV could respectively be assigned to Fe^{2+} and Fe^{3+} $2p_{3/2}$, while those at 724.5 and 727.4 eV could respectively be assigned to Fe^{2+} and Fe^{3+} $2p_{1/2}$, and those at 718.7 and 732.9 eV could respectively be assigned to Fe^{2+} and Fe^{3+} shake-up satellites.[26] It was illustrated that Fe^{2+} and Fe^{3+} co-existed on the surface of WAC. The Fe^{3+}/Fe^{2+} molar ratios on the surface of Fe/WACs were presented in Table 3. With increasing Fe content, the Fe^{3+}/Fe^{2+} molar ratios on the surface decreased from 0.63 to 0.50 gradually, although the Fe^{3+}/Fe^{2+} molar ratio was controlled to be 2/1 in the preparation process. It implied that with increasing Fe content, the distribution of Fe^{2+} on the surface was enhanced. As similar XRD patterns were attained with different Fe content, the above data indicated that the formation of iron oxide species on all Fe/WACs was similar.

Fig. 4 and 5 exhibited the C 1s and O 1s spectra of the six samples, respectively. Both the C 1s and O 1s spectra of all samples were asymmetric, indicating the convolution of different surface oxygen and carbon species.[27] The surface carbon species of all samples should be assigned to graphite carbon and contaminant carbon,

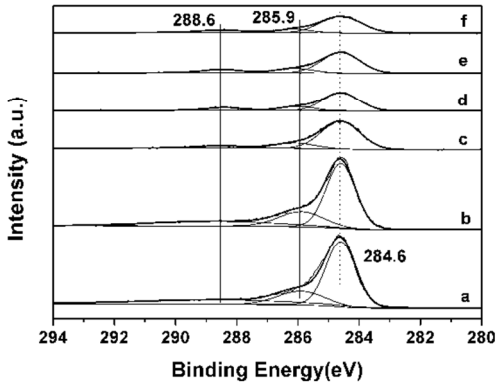

Fig. 4 C1s spectra of catalysts: (a) WAC, (b) Fe/WAC/0.89, (c) Fe/WAC/2.76, (d) Fe/WAC/4.82, (e) Fe/WAC/6.55, (f) Fe/WAC/6.94.

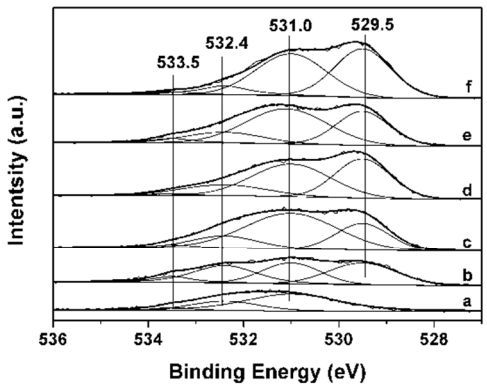

Fig. 5 O1s spectra of catalysts: (a) WAC, (b) Fe/WAC/0.89, (c) Fe/WAC/2.76, (d) Fe/WAC/4.82, (e) Fe/WAC/6.55, (f) Fe/WAC/6.94.

phenol carbon, and carboxylic carbon according to the binding energy of 284.6, 286.0, and 288.6 eV, respectively, after deconvolution.[28] The surface oxygen species of WAC should be assigned to carbonyl oxygen, phenol oxygen, and carboxylic oxygen according to the binding energy of 531.0, 532.4 and 533.5 eV, respectively.[27] It was notable that the O1s peaks (529.5 eV) in Fe/WACs spectra appeared and shifted to lower binding energy with broadening with respect to that of WAC, which was characteristic of Fe-O in iron oxide species.[29] The peaks at 288.6 and 533.5 eV had a declined trend with the increase of Fe content. It implied that iron ions might combine with carboxylic groups in the preparation process. The results were consistent with that of Zhang et al.[30] Additionally, Fe^{3+} and Fe^{2+} might interact strongly with surface oxygen functional groups, which could inhibit the formation of crystal Fe_3O_4. The chemical compositions of the samples in atomic percentage were shown in Table 3. As seen, the Fe and O atomic percentage increased with increasing Fe content, but the Fe/O atomic ratio kept nearly invariable. Based on the above data, we could not confirm the formation of any kind of crystal iron oxide species.

Table 4 Effect of Fe content of the catalysts for the hydroxylation of phenol [a]

Catalyst	X_{Ph} (%)	S_{DHB} (%)	Y_{DHB} (%)	Yield of product (%)				$U_{H_2O_2}$ (%)	TOF (h-1) [b]
				CAT	HQ	BQ	Others		
Blank	0	0	0	0	0	0	0	-	-
WAC	4.6	76.1	3.5	2.7	0.8	1.1	0	5.5	-
Fe/WAC/0.89	25.5	67.5	17.2	9.3	7.9	3.3	5.0	23.8	245.5
Fe/WAC/2.76	37.6	76.6	28.8	16.1	12.7	3.3	5.5	35.4	116.7
Fe/WAC/4.82	43.3	78.5	34.0	18.9	15.1	2.1	7.2	38.2	77.0
Fe/WAC/6.55	51.1	80.6	41.2	22.0	19.2	1.7	8.2	44.6	66.9
Fe/WAC/6.94	51.7	80.3	41.5	21.9	19.6	1.1	9.1	43.7	63.8

[a] Reaction condition: 0.05 g of catalyst, 0.48 g of phenol (5 mmol), 0.50 g of 30 wt% aqueous H_2O_2 (5 mmol), 10 ml water, reaction temperature 313 K, reaction time 40 min. [b] Turnover frequency (TOF) = moles of phenol converted per mole of Fe in the catalyst per hour.

Table 5 Control experiments for the hydroxylation of phenol [a]

Catalyst	Time (min)	X_{Ph} (%)	S_{DHB} (%)	Y_{DHB} (%)	Yield of product (%)			
					CAT	HQ	BQ	Others
Fe/WAC/6.55 [b]	5	22.1	57.9	12.8	7.5	5.3	3.3	6.0
Leachate [b]	60	23.0	51.7	11.9	7.0	4.9	4.3	6.8
Solid catalyst [c]	40	50.5	71.3	40.0	21.5	18.5	1.6	12.9
Leachate [c]	40	35.4	56.5	20.0	11.5	8.5	2.2	13.2

[a] Reaction condition: 0.05 g of Fe/WAC/6.55, 0.48 g of phenol (5 mmol), 0.50 g of 30 wt% aqueous H_2O_2 (5 mmol), 10 ml of water, reaction temperature 313 K. [b] from the first control experiment. [c] from the second control experiment.

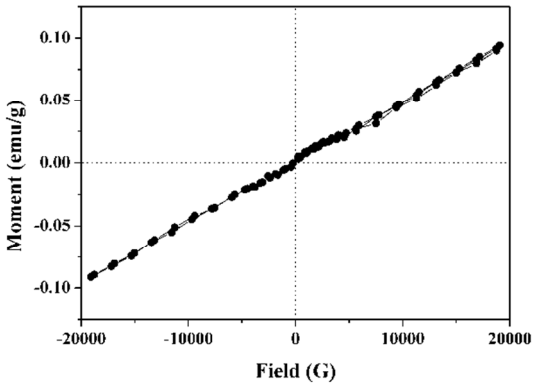

Fig. 6 Magnetic hysteresis loop of the Fe/WAC/6.55.

3.1.5 Magnetic properties

To detect if Fe_3O_4 was formed, magnetic property of Fe/WAC/6.55 was measured. As shown in Fig. 6, the average saturation magnetization of Fe/WAC/6.55 was 0.09 emu/g. Compared to the values reported, that is, 0.53 emu/g for Fe/WAC-400 by Jin et al.[2] , 5.73 emu/g for C-Fe-750-1.0 by Zhang et al.[31] and 63.5 emu/g for Fe_3O_4 nanoparticles[32], it was too weak to confirm the formation of Fe_3O_4 species. It could be caused by the fact that Fe content of the catalysts used in the present work was comparatively low to that of Fe/WAC-400 and Fe_3O_4 nanoparticles.

3.1.6 The DR UV-vis and FTIR analysis

DR UV-vis was used to characterize the catalysts (Fig. S1†). The spectra of Fe/WAC/0.89 and 2.76 showed little variation compared to that of WAC. With increase of Fe content, the intensity of a broad peak at the scope of 300-500 nm became strong. It implied that the broad peak should be attributed to iron oxide species. Liang et al. proposed that the peaks at about 333 and 427 nm were assigned to octahedral complex of iron and Fe^{3+} in small oligomeric Fe_xO_y clusters.[20]

FTIR spectra were shown in Fig. S2†. The intensity of the bands at 1300-900 cm^{-1} corresponded to C-O stretching[33] was weakened with increasing Fe content. Similarly, the intensity of the bands at 1384 cm^{-1} corresponded to COO^- stretching[34] was weakened with increasing Fe content. The results were consistent with that of XPS. It implied that iron species could combine with carboxylic groups.

3.1.7 The HRTEM analysis

The HRTEM characterizations have been carried out, and the results were shown in Fig. S3†. HRTEM profiles clearly showed how the iron dispersion varied,[35] which was in the sense: Fe/WAC/0.89 > Fe/WAC/6.55. With increasing Fe content, the catalyst exhibited a slightly worse Fe dispersion. The results were consistent with those obtained by XRD. On the other hand, no obvious crystal iron oxide species were found in the images of C and D. It implied that the iron oxide species was amorphous on the catalysts. Correspondingly, the peak at about 35.6° was a broad peak in XRD patterns. Thus, the increase of diffraction peak intensity with increasing Fe content was related to the formation of more iron oxides.

3.2 Catalytic phenol hydroxylation

3.2.1 Effect of Fe content of the catalyst

Liquid hydroxylation of phenol catalyzed by Fe/WACs using H_2O_2 as oxidant had been studied. The catalytic performances of various catalysts in the hydroxylation of phenol were presented in Table 4. The result of blank experiment exhibited that H_2O_2 alone was unable

to oxidize phenol to a significant extent in the absence of the catalyst, especially at low temperature (313 K).[1] Moreover, X_{Ph} and S_{DHB} were very low on pure WAC. After Fe/WACs were added, a remarkable increase in the X_{Ph} was observed.

To further verify the heterogeneous character of the catalyst, two control experiments were operated. In the first control experiment, the reaction was carried out over Fe/WAC/6.55 under the same reaction conditions. After 5 min, the catalyst was removed, but the reaction kept on going until 60 min. The results were presented in Table 5. It indicated that after removal of catalyst, the hydroxylation of phenol could not continue to be conducted. In the second control experiment, only 0.05 g of Fe/WAC/6.55 and solvent (H_2O and acetic acid) were used to carry out the reaction at 40 ^oC for 40 min. Then the mixture was taken out and filtered. The solid catalyst and leachate were obtained and used to catalyze the phenol hydroxylation under the same conditions, respectively. As shown in Table 5, the activity of the solid catalyst was almost the same as the fresh catalyst (X_{Ph}: 50.5% *vs* 51.1%), whereas the leachate showed much smaller activity than the fresh catalyst (X_{Ph}: 35.4% *vs* 51.1%). The results above demonstrated that the reaction was mainly catalyzed by iron oxide particles on the surface of the heterogeneous catalyst. An additional experiment was carried out to identify the iron species leached. Small amount of aqueous solution of KSCN was added into the leachate from the second control experiment, and the solution turned to be light red. It indicated that tiny Fe^{3+} existed in the leachate. Then the pH of leachate was adjusted to 5, centrifuged, and bromine water was added into the supernatant. Small amount of aqueous solution of KSCN was added, no red color appeared. These results indicated that Fe^{3+} was inclined to leach.

To work out what is the true active phase for the hydroxylation of phenol, five catalysts were prepared with different molar ratios of Fe^{3+} to Fe^{2+} (0/1, 1/1, 3/1, 4/1, 1/0) but identical total iron content (6.55 wt%) through the same preparation process. Under the optimized conditions, the catalytic activity was tested, the results were shown in Table S1†. The results showed that the changes of molar ratio of Fe^{3+} to Fe^{2+} had little effect on the activity of titled reaction. But Fe^{3+} or Fe^{2+} alone on the catalysts exhibited only low catalytic activity. It implied that the true active phase for phenol hydroxylation was the cooperation of the two Fe species, nothing with the difference of Fe^{3+} or Fe^{2+} amount. It was found that Fe^{3+} species was easier to leach than Fe^{2+} species above all. This led us to suspect that the binding of Fe^{2+} species with WAC surface was stronger and the attachment of Fe^{2+} was prior to Fe^{3+} on WAC considering the saturation of Fe species on WAC surface. There would be enough Fe^{2+} interacted with WAC forming the catalyst which satisfied the demand of phenol hydroxylation in the series of control experiments, even though the proportion of Fe^{2+} was relative low. That is to say, the variation of Fe^{3+}/Fe^{2+} ratios within the experiments did not make significant changes of the surface Fe species on WAC. This was why no relation was observed between the amount of Fe^{2+} and that of Fe^{3+} in the impregnation solution.

The X_{Ph} and S_{DHB} increased with increase of Fe content from 0.89 to 6.55 wt% respectively and reached a maximum (51.1% and 80.6%) at 6.55 wt%. When the Fe content increased further from 6.55 to 6.94 wt%, the X_{Ph} and S_{DHB} kept almost invariant, which was likely attributed to the saturation of Fe content of catalysts. Due to the fact

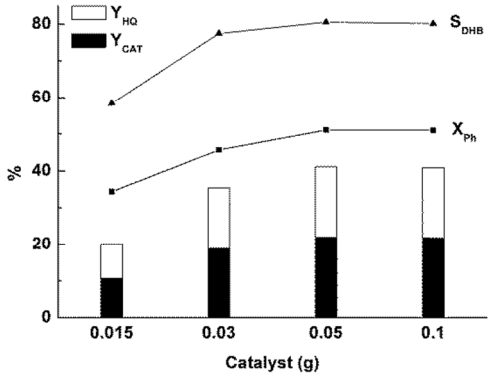

Fig. 7 Effect of catalyst amount for the hydroxylation of phenol [a] [a] Reaction condition: Fe/WAC/6.55, 0.48 g of phenol (5 mmol), 0.50 g of 30 wt% aqueous H_2O_2 (5 mmol), 10 ml of water, reaction temperature 313 K, reaction time 40 min.

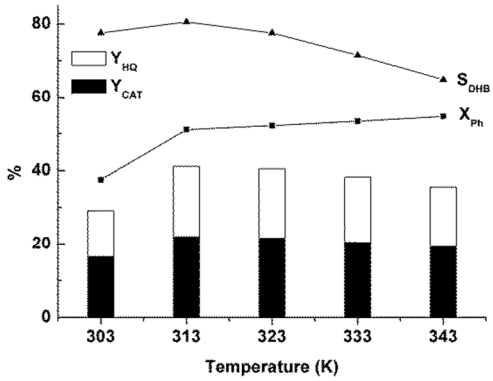

Fig. 8 Effect of reaction temperature for phenol hydroxylation [a] [a] Reaction condition: 0.05 g of Fe/WAC/6.55, 0.48 g of phenol (5 mmol), 0.50 g of 30 wt% aqueous H_2O_2 (5 mmol), 10 ml of water, reaction time 40 min.

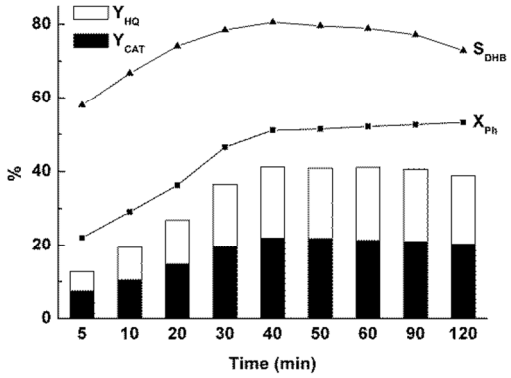

Fig. 9 Effect of reaction time for the hydroxylation of phenol [a] [a] Reaction condition: 0.05 g of Fe/WAC/6.55, 0.48 g of phenol (5 mmol), 0.50 g of 30 wt% aqueous H_2O_2 (5 mmol), 10 ml of water, reaction temperature 313 K.

Table 6 Effect of phenol/H_2O_2 molar ratio for phenol hydroxylation [a]

Phenol/H_2O_2 (molar ratio)	X_{Ph} (%)	S_{DHB} (%)	Y_{DHB} (%)	Yield of product (%)				$U_{H_2O_2}$ (%)
				CAT	HQ	BQ	Others	
1:2	80.2	45.3	36.3	19.9	16.4	1.6	42.3	19.8
1:1.5	65.5	58.6	38.4	20.6	17.8	1.6	25.5	27.7
1:1	51.1	80.6	41.2	22.0	19.2	1.7	8.2	44.6
1:0.66	40.4	71.8	29.0	15.5	13.5	1.7	9.7	49.1
1:0.33	30.5	53.4	16.3	8.8	7.5	1.6	12.6	59.1

[a] Reaction condition: 0.05 g of Fe/WAC/6.55, 0.48 g of phenol (5 mmol), 10 ml of water, reaction temperature 313 K, reaction time 40 min.

Table 7 Effect of catalyst recycling on the hydroxylation of phenol [a]

Catalyst	X_{Ph} (%)	S_{DHB} (%)	Y_{DHB} (%)	Yield of product (%)				Fe content (wt%)
				CAT	HQ	BQ	Others	
BR[b]	51.1	80.6	41.2	22.0	19.2	1.7	8.2	6.55
AR1[c]	50.5	71.3	40.0	21.5	18.5	1.6	12.9	6.04
AR2	47.4	69.2	36.8	19.4	17.4	1.8	12.8	5.47
AR3	45.8	67.7	35.1	18.1	17	2.1	12.7	4.83

[a] Reaction condition: 0.05 g of Fe/WAC/6.55, 0.48 g of phenol (5 mmol), 0.50 g of 30 wt% aqueous H_2O_2 (5 mmol), 10 ml of water, reaction temperature 313 K, reaction time 40 min. [b] BR meant before reaction. [c] AR1 meant after once run, ARN means after N times run.

that iron oxide species loaded on Fe/WACs were in a similar form, the increase of activity might be mainly caused by the increase of active iron oxide species. Under the same conditions, Fe/WAC/6.55 gave the best activity, with 51.1% of X_{Ph}, 80.6% of S_{DHB}, 41.2% of yield to DHB and 44.6% of $U_{H_2O_2}$, which were higher than those reported in literatures[2,8]. On the other hand, the method used for the calculation of TOF value was based on the total Fe content, whereas only part of Fe was exposed and accessible for reactants. Thus, the calculated of TOF value was smaller than the actual value. Although the moles of phenol converted increased with increasing total Fe content in the catalyst, but the moles of total Fe increased was more than that of phenol converted in the same time. So the TOF value calculated decreased. Especially, 66.9 h^{-1} of TOF on Fe/WACs was much higher than the values (13.0 h^{-1} or smaller) reported in literatures[2,36,37].

It was found that the selectivity of CAT was higher than HQ. There were many similar reports about the same phenomenon[1,2,8]. Mugo et al.[38] suggested that the predominance of CAT was expected for metal-mediated hydroxylation occurring via a pathway involving initial weak coordination of both phenol and H_2O_2 to the active site. The anchoring of the two reactants in close proximity to each other led predominantly to a cis arrangement, which in turn resulted in ortho-substitution of the phenol. On the other hand, our previous studies found that the aromatic compounds had predominant selectivity to ortho-hydroxylated products over Fe/AC catalyst.[39]

3.2.2 Effect of catalyst amount

The effect of the catalyst amount on the variation of activity was shown in Fig. 7. It was observed that from 0.015 to 0.05 g, the X_{Ph} and S_{DHB} enhanced. From 0.05 to 0.1 g, the X_{Ph} and S_{DHB} kept nearly invariant. When the amount of catalyst was 0.015 g, iron oxide species, which acted as active center, were not enough to simultaneously activate phenol and H_2O_2 effectively, resulting in low activity. When the amount of catalyst was greater than or equal to 0.05 g, iron oxide species were enough to simultaneously activate phenol and H_2O_2, and hence the X_{Ph} and S_{DHB} kept almost invariant. It also indicated that excess amount of catalyst gave no more benefits to promote the phenol hydroxylation. For cost saving, 0.05 g was chosen as the optimal catalyst amount.

3.2.3 Effect of reaction temperature

The effect of reaction temperature was presented in Fig. 8. From 303 to 343 K, the X_{Ph} increased from 37.5% to 54.7% correspondingly. While the S_{DHB} increased firstly, reached the maximum (80.6%) at 313 K, and then decreased. It was suggested that the increase of reaction temperature was beneficial to enhance the X_{Ph}, but disadvantageous to improve the S_{DHB}.[1] Moreover, according to the Arrhenius law, an increase in reaction temperature should result in an increase of reaction rate. On the other hand, an increase in reaction temperature would accelerate the decomposition of H_2O_2, which was disadvantageous to the target reaction. Therefore, the insignificant changes in the X_{Ph} detected above 313 K could be attributed to the decomposition of H_2O_2.[1] Similar observation had been reported for other iron containing catalysts.[40] Thus, 313 K was the optimal temperature for the hydroxylation of phenol over Fe/WAC/6.55. The same trend was also reported by Choi et al.[40] over Fe-MCM-41 catalyst, other than that reported by Jin et al.[2] over Fe/AC catalyst. Furthermore, from the energy consumption and safety perspective, the optimized reaction temperature (313 K) in this work was more favorable than those (343 K or higher) reported in literatures.[8, 10]

3.2.4 Effect of reaction time

The dependence of catalytic activity on the reaction time was shown in Fig. 9. A pronounced induction period was not observed at the beginning of the reaction. From 5 to 40 min, the X_{Ph} and S_{DHB} were increased from 22.1% to 51.1% and from 57.9% to 80.6%, respectively. From 40 to 120 min, the X_{Ph} slightly increased, but the S_{DHB} slightly decreased. The result was consistent with that reported by Shi et al.[1]

The decomposition behavior of H_2O_2 was investigated from 0 to 150 min and the results were shown in Fig. S4†. The results showed that the decomposition of H_2O_2 on WAC was slower than that on Fe/WAC/6.55. It implied that the decomposition of H_2O_2 was enhanced with loading Fe species.

As shown in Fig. S4†, about 30% of H_2O_2 was decomposed at 40 min in blank experiment. The invariant character of the X_{Ph} should be related to partly degradation of H_2O_2 and the blocking of active sites by products or tars. The decrease of S_{DHB} from 40 to 120 min might be resulted by the fact that the anticipated products were deep oxidized, and the Y_{HQ} and Y_{CAT} decreased within over-long reaction time. Consequently, the optimal reaction time was 40 min, which was shorter than that over most of the catalysts available for the production of CAT and HQ (about 6 h).[41]

3.2.5 Effect of phenol/H_2O_2 molar ratio

The reaction was carried out with varying amount of H_2O_2 to a fixed amount of phenol from 1:2 to 1:0.33 (phenol/H_2O_2 molar ratios). It was observed from Table 6 that the X_{Ph} was higher at a lower phenol/H_2O_2 molar ratio, because the higher dose of H_2O_2 meant greater generation of hydroxyl radicals.[1] With the variation of phenol/H_2O_2 molar ratio from 1:2 to 1:0.33, the S_{DHB} increased firstly, achieved the highest value (80.6%) at 1:1, and then decreased. At the molar ratio of 1:2, the amount of H_2O_2 was excessive, undesirable H_2O_2 self-decomposition and deep oxidation of DHB producing tars might be serious, consequently the S_{DHB} was very low. At the molar ratio of 1:1, the production of reactive species from both phenol and H_2O_2 were proper, so the highest S_{DHB} was obtained. At the molar ratio of 1:0.33, the amount of H_2O_2 was too small to produce enough reactive species to combine with that from phenol; hence link-coupled compounds were produced leading to numerous tar generation, whereas the yield of others increased, leading to the decrease of the S_{DHB}. The results were consistent with those reported in literatures[2,20]. It should be noted that this variation tendency was different from other reports[18,42]. The inconsistency might stem from the fact that in different reports[18,42], the actual concentration of H_2O_2 in the solution was different. Additionally, the $U_{H_2O_2}$ gradually increased with the molar ratio of phenol/H_2O_2 varied from 1:2 to 1:0.33. It was caused by the fact that a part of H_2O_2 decomposed into water and oxygen at high concentrations of H_2O_2. Therefore, it was conservatively concluded that the optimal molar ratio of phenol/H_2O_2 was 1:1.

3.2.6 Catalyst recycling

Considering the economic benefits, the reusability of the catalyst was investigated. The favorable Fe/WAC/6.55 was used 4 runs for the target reaction. After every reaction, the catalyst was separated by filtration, washed with deionized water and acetonitrile several times, dried at ambient temperature, and reused for fresh reaction mixture. All the 4 runs were carried out under the same conditions, however, the X_{Ph} and S_{DHB} decreased partly from 51.1% to 45.8% and from 80.6% to 67.7%, respectively, as presented in Table 7.

It was well-known that the main limitation of using Fe as the active metal was the leaching of active species from solid to solution.[21] The Fe content of Fe/WAC/6.55 before and after reaction were detected by ICP-AES, and listed in Table 7. It was observed that there was low level leaching occurred in every reaction, which could be the partial reason for catalyst deactivation. On the other hand, tars, which was found during the tests performed, successively deposited on the surface and blocked active sites.[20]

The catalytic stability of Fe/WAC/0.89 was also investigated, and the results were shown in Table S2†. Under the same conditions, the X_{Ph} and Fe content decreased from 25.5% to 5.0% and from 0.89 to 0.51 wt%, respectively. A small amount of leaching of Fe did not significantly affect its catalytic performance in the second run. The decrease of activity of AR2 and 3 (Table S2) should be mainly attributed to the deposition of tars on the catalyst surface, which blocked active sites. In brief, the leaching of a small amount of Fe might not be the main reason for the reduction of the catalytic performance. Although the presence of carbon support excluded regeneration by calcination, the high activity and simple preparation process made Fe/WACs potential for phenol hydroxylation. It was interesting to study the regeneration of the catalyst by other methods instead of calcination.

4 Discussions

Because Fe_3O_4 on AC was found to be active for phenol hydroxylation,[2] we envisaged to prepare supported Fe_3O_4 species by impregnation-co-precipitation method. However, the results did not support the formation of crystal Fe_3O_4 on the surface of WAC by XRD and magnetic measurement. Only the co-existence of Fe^{2+} and Fe^{3+} on the surface of WAC was confirmed. The control experiments implied that the cooperation of two iron oxide species were the true active phase for titled reaction. Although the average saturation magnetization of Fe/WAC/6.55 was smaller than those of Fe/AC-400 and C-Fe-750-1.0 respectively, Fe/WAC/6.55 gave higher activity under similar conditions. The possible reasons were the followings. First, the desirable Fe_3O_4 species might not be generated, while the phenol hydroxylation reaction required only the co-existence of iron oxide species (Fe^{2+} and Fe^{3+}) with a proper arrangement. In the present work, the arrangement of Fe^{2+} and Fe^{3+} on WAC satisfied the demand of phenol hydroxylation. Second, the Fe_3O_4 species might be generated. However, it was difficult to be detected by the magnetic measurement because of the high dispersion. In brief, few iron oxide species on the surface of catalyst offered favorable activity of phenol hydroxylation.

5 Conclusions

Fe/WACs were successfully prepared by impregnation-co-precipitation method for phenol hydroxylation with H_2O_2 as oxidant. It was confirmed that Fe^{2+} and Fe^{3+} with a proper arrangement co-existed on WAC. The cooperation of two species could be the active phase for phenol hydroxylation. With the increase of concentration of iron ions in the preparation process, iron oxide species were saturated gradually on WAC. The thus-obtained Fe/WACs satisfied the demand on phenol hydroxylation. Among all the investigated catalysts, Fe/WAC/6.55 showed the highest catalytic activity with 51.1% of conversion of phenol and 80.6% of selectivity to DHB. The yield of DHB obtained was 41.2%. Fe/WACs acting as efficient

solid catalysts exhibited promised in industrial applications with its low cost, benignity to the environment, and preparation convenience.

Acknowledgements

The project is financially supported by the National Natural Science Foundation of China (Nos. 20502017, 20872102), and the characterization of the catalyst from the Analytic and Testing Center of Sichuan University is greatly appreciated. The suggestions by the reviewers are also gratefully accepted.

Notes and references

Key Laboratory of Green Chemistry and Technology, Ministry of Education, College of Chemistry, Sichuan University, Chengdu, Sichuan, 610064, China. Tel: +86-28-85411105; Fax: +86-28-85411105; E-mail: G. Y. Li: gchem@scu.edu.cn, C. W. Hu: changweihu@scu.edu.cn

* The author was corresponding authors.

1 F. Shi, L. Mu, P. Yu, J. Hu and L. Zhang, *J. Mol. Catal. A: Chem.*, 2014, **391**, 66.
2 M. Jin, R. Yang, M. Zhao, G. Li and C. Hu, *Ind. Eng. Chem. Res.*, 2014, **53**, 2932.
3 H. Jiang, X. Jiang, F. She, Y. Wang, W. Xing and R. Chen, *Chem. Eng. J.*, 2014, **239**, 373.
4 D. P. Ivanov, L. V. Pirutko and G. I. Panov, *J. Catal.*, 2014, **311**, 424.
5 P. S. Niphadkar, M. S. Kotwal, S. S. Deshpande, V. V. Bokade and P. N. Joshi, *Mater. Chem. Phys.*, 2009, **114**, 344.
6 R. Dimitrova, M. Spassova, *Catal. Commun.*, 2007, **8**, 693.
7 H.-C. Jeong, I.-W. Shim, K. Y. Choi, J. K. Lee, J. -N. Park and C. W. Lee, *Korean J. Chem. Eng.*, 2005, **22**, 657.
8 S. Yang, G. Liang, A. Gu and H. Mao, *Appl. Surf. Sci.*, 2013, **285**, 721.
9 H. Zhang, C. Tang, Y. Lv, C. Sun, F. Gao, L. Dong and Y. Chen, *J. Colloid Interf. Sci.*, 2012, **380**, 16.
10 B. Li, J. Xu, J. Liu, S. Zuo, Z. Pan and Z. Wu, *J. Colloid Interf. Sci.*, 2012, **366**, 114.
11 Y. Jiang, K. Lin, Y. Zhang, J. Liu, G. Li, J. Sun and X. Xu, *Appl. Catal. A: Gen.*, 2012, **445-446**, 172.
12 S. Kannan, *Catal. Surv. Asia*, 2006, **10**, 117.
13 S. Kannan, A. Dubey and H. Knozinger, *J. Catal.*, 2005, **231**, 381.
14 C. A. S. Barbosa, P. M. Dias, A. M. d. C. Ferreira and V. R. L. Constantino, *Appl. Clay Sci.*, 2005, **28**, 147.
15 C. K. Modi, P. M. Trivedi, *Microporous Mesoporous Mater.*, 2012, **155**, 227.
16 X. Tan, Y. Zhao, G. Li and C. Hu, *Appl. Surf. Sci.*, 2011, **257**, 6256.
17 E. A. Karakhanov, A. L. Maximov, Y. S. Kardasheva, V. A. Skorkin, S. V. Kardashev, V. V. Predeina, M. Y. Talanova, E. Lurie-Luke, J. A. Seeley and S. L. Cron, *Appl. Catal. A: Gen.*, 2010, **385**, 62.
18 S. Li, G. Li, G. Li, G. Wu and C. Hu, *Microporous Mesoporous Mater.*, 2011, **143**, 22.
19 F. Adam, J.-T. Wong and E.-P. Ng, *Chem. Eng. J.*, 2013, **214,** 63.
20 X. Liang, R. Yang, G. Li and C. Hu, *Microporous Mesoporous Mater.*, 2013, **182**, 62.
21 S. Navalon, A. Dhakshinamoorthy, M. Alvaro and H. Garcia, *ChemSusChem*, 2011, **4**, 1712.
22 H. Li, D. Yu, Y. Hu, P. Sun, J. Xia and H. Huang, *Carbon*, 2010, **48**, 4547.
23 S. Yan, X. Zhang, Y. Sun, T. Wang, X. Chen and J. Yin, *Colloid Surface B*, 2014, **113**, 302.
24 S. A. Kulkarni, P.S. Sawadh, P. K. Palei and K. K. Kokate, *Ceram. Int.*, 2014, **40**, 1945.
25 A. Gervasini, C. Messi, P. Carniti, A. Ponti, N. Ravasio and F. Zaccheria, *J. Catal.*, 2009, **262**, 224.
26 A. D. Stefanis, S. Kaciulis and L. Pandolfi, *Microporous Mesoporous Mater.*, 2007, **99**, 140.
27 Y. Zhong, G. Li, L. Zhu, Y. Yan, G. Wu and C. Hu, *J. Mol. Catal. A: Chem.*, 2007, **272**, 169.
28 X.-L. Wu, L. Wang, C.-L. Chen, A.-W. Xu and X.-K. Wang, *J. Mater. Chem. Phys.*, 2011, **21**, 17353.
29 A. P. Grosvenor, B. A. Kobe, M. C. Biesinger and N. S. McIntyre, *Surf. Interface Anal.*, 2004, **36**, 1564.
30 L. Zhang, H. Liu, G. Li and C. Hu, *Chin. J. Chem. Phys.*, 2012, **25**, 585.
31 X. Zhang, Y. Li, G. Li and C. Hu, *RSC adv.*, 2015, **5**, 4984.
32 S. A. Kulkarni, P. S. Sawadh, P. K. Palei and K. K. Kokate, *Ceram. Int.*, 2014, **40**, 1945.
33 S. Khorramfar, N. M. Mahmoodi, M. Arami and H. Bahrami, *Desalination*, 2011, **279**, 183.
34 C. Moreno-Castilla, M. V. Lopez-Ramon and F. Carrasco-Marın, *Carbon*, 2000, **38**, 1995.
35 F. M. Duarte, F. J. Maldonado-Hódar and L. M. Madeira, *Appl. Catal. A: Gen.*, 2013, **458**, 39.
36 S. F. Mapolie, J. L. v. Wyk, *Inorganica Chimica Acta*, 2013, **394**, 649.
37 A. Kumar, D. Srinivas, *J. Mol. Catal. A: Chem.*, 2013, **368-369**, 112.
38 J. N. Mugo, S. F. Mapolie and J. L. v. Wyk, *Inorganica Chimica Acta,* 2010, **363**, 2643.
39 Y. Zhong, G. Li, L. Zhu, D. Tang and C. Hu, *Chem. J. Chinese U.,* 2007, **28**, 1570.
40 J.-S. Choi, S.-S. Yoon, S.-H. Jang and W.-S. Ahn, *Catal. Today*, 2006, **111**, 280.
41 H. S. Abbo, S. J. J. Titinchi, *Appl. Catal. A: Gen.*, 2012, **435-436**, 148.
42 G. Zhang, J. Long, X. Wang, Z. Zhang, W. Dai, P. Liu, Z. Li, L. Wu and X. Fu, *Langmuir*, 2010, **26**, 1362.